APPENDIX A

VISIBILITY MAPS DERIVED FROM MEASURED AND SPATIALLY INTERPOLATED IMPROVE AND CDN DATA

Because the majority of Class I areas with IMPROVE monitoring are located in the western United States, spatial coverage of the IMPROVE network is sparse in the eastern United States. As a result, maps of a visibility index, such as the light extinction coefficient (b_{ext}) or deciview (dv) based on IMPROVE data [Malm *et al*., 1994; Sisler, 1996; Sisler *et al*., 1993; Chapter 3.2.2] lack spatial resolution in the eastern United States, where visibility conditions are traditionally the worst.

High-resolution maps of b_{ext} derived from airport visual range observations are available [Falke and Husar, 1998]. While these maps have detailed spatial resolution, they have limitations due to the human observation method from which they are derived. For example, the observationally based b_{ext} estimates are truncated at a minimum threshold and the observer system on which these maps are based is no longer widely used in the United States, rendering observationally based b_{ext} maps obsolete for future trend analysis. In contrast, b_{ext} reconstructed from aerosol mass concentration data can be used to estimate visibility conditions on the cleanest and haziest conditions, and these data can be combined with future monitoring for long-term trend analyses. Perhaps the greatest advantage of b_{ext} maps reconstructed from aerosol mass concentration data, over those estimated from visual range, is reconstructed aerosol b_{ext} allows for apportionment of visibility impairment to specific aerosol species.

In this section, IMPROVE and the CASTNet Deposition Network (CDN) data are combined to show spatial patterns in mean sulfate and nitrate mass concentration, as well as reconstructed b_{ext}, across the contiguous United States. The particle sulfate and nitrate maps represent mass concentrations reported by two networks, while the visibility maps are derived using the IMPROVE algorithm to reconstruct b_{ext} [Chapter 3.1]. Because routine CDN sampling protocol does not include measurements of all chemical species necessary to reconstruct b_{ext}, concentrations at CDN monitoring locations for species other than sulfates and nitrates are estimated by spatial interpolation of IMPROVE data.

In using the deposition network data as a surrogate for IMPROVE data in the b_{ext} algorithm, we adopt the assumption that sulfates and nitrates are responsible for the majority of light extinction at most CDN monitoring locations, particularly in the eastern United States where spatial coverage of IMPROVE sites is sparse. If chemical species other than sulfates and nitrates constitute a large portion of the extinction budget at a CDN site, then the point estimated b_{ext} will

rely heavily on interpolated IMPROVE fields and will contain uncertainties associated with the interpolation. However, in support of our underlying assumption, sulfates (as ammonium sulfate) contribute 70% or more to the annual average particle b_{ext} in the eastern United States based on IMPROVE data, while the contribution of other chemical species to the extinction budget is approximately 10% or less [Chapter 3.2.1]. Particle nitrates can also play a significant role in visibility reduction. For example, nitrates contribute approximately 30% to annual particle b_{ext} near some IMPROVE sites in southern California [Chapter 3.2.2]. CDN data shown in this section indicate high wintertime particle nitrate mass concentrations throughout large urban and agricultural regions of the Midwest, which may indicate nitrates are major contributors to the particle light extinction budget in that region during the cold season.

Before using CDN particle sulfate and nitrate mass concentrations as surrogates for IMPROVE protocol measurements, we compared the respective data sets. Results from this comparison show mean sulfate mass concentrations are comparable, however, bias between particle nitrate mass concentrations are observed at many nearby sites from the respective networks [Ames and Malm, 2000; Appendix G]. Field comparisons have shown good agreement between sulfate, although particle nitrate mass concentrations measured by CDN samplers, which use Teflon substrates to collect particles, may be underestimated by about 10% [Clean Air Status and Trends Network, 1998] compared to measurements from collocated samplers that collect particle nitrate on denuded nylon substrates. Other comparison studies have reported particle nitrate undersampling, attributed to particle nitrate volatilization from Teflon filters, of 60% during the summer, and 30% on an annual basis [Chow et al., 1994; Hering and Cass, 1999]. If particle nitrate volatilization occurs in the CDN samplers, then particle nitrate mass concentrations reported by that network may be a lower-bound estimate of the true ambient mass concentration. On the other hand, particle nitrate mass concentrations reported by the CDN may overestimate fine particle nitrate as measured by IMPROVE protocol samplers if measurable particle nitrate mass resides in the coarse mode.

A.1 METHOD

Reconstructed b_{ext} is calculated using data from the three-year period December 1995 through November 1998, and for the summer (June, July, August) and winter (December, January, February) seasons during that time period. The b_{ext} reconstruction follows the method in Chapter 3.1. All b_{ext} values in this section refer to mean aerosol b_{ext}. IMPROVE sulfate mass concentration is estimated from module A elemental S. Descriptions of the IMPROVE sampling modules, the chemical species that they collect, and related analytical methods are given in Chapter 2.1. CDN sulfate and nitrate ion mass concentrations are obtained from Teflon substrates. Hourly relative humidity (RH) measurements at IMPROVE and CDN sites are averaged following the method outlined in Chapter 3.1, and the relative humidity correction factor (F_T(RH)) is determined using Equation 3.7 and appropriate coefficients for seasonal or season weighted annual mean RH at all IMPROVE and CDN sites.

A minimum 70% of the possible measurements is required to calculate the mean particle mass concentration at any site for the three-year and summer periods, and a minimum of 60% is required for the winter period. Tallying sites in the combined IMPROVE/CDN data set shows 123 sites meet the valid data requirement for sulfate during the three-year period (60 IMPROVE,

63 CDN). Figure A.1 is a map showing the corresponding site abbreviations, and Table A.1 lists the site abbreviations, the state where the monitoring sites reside, and site names. Fifty IMPROVE and 63 CDN sites meet minimum data requirement for particle nitrate during the three-year period. The number of sites meeting the minimum data requirement for winter and summer periods is similar to those for the three-year period. A minimum of 50% valid data is required to calculate seasonal RH.

The criteria to calculate b_{ext} at any monitoring site is that sufficient sulfate measurements are available to calculate a mean for the desired time period. To calculate b_{ext} at sites where chemical concentration data other than sulfate are missing, available species mass concentration data are interpolated to a 0.5 degree latitude/longitude grid across the contiguous United States, and data are taken from the nearest grid value. Generally, data missing are at CDN sites for species other than sulfate and nitrate, for which species mass concentrations are taken from interpolated IMPROVE data. However, some interpolated data are used at IMPROVE sites without either of sampling modules B, C, or D. For example, interpolated particle nitrate mass concentrations derived from the combined data set are used at IMPROVE sites operating without module B which collects particle nitrate.

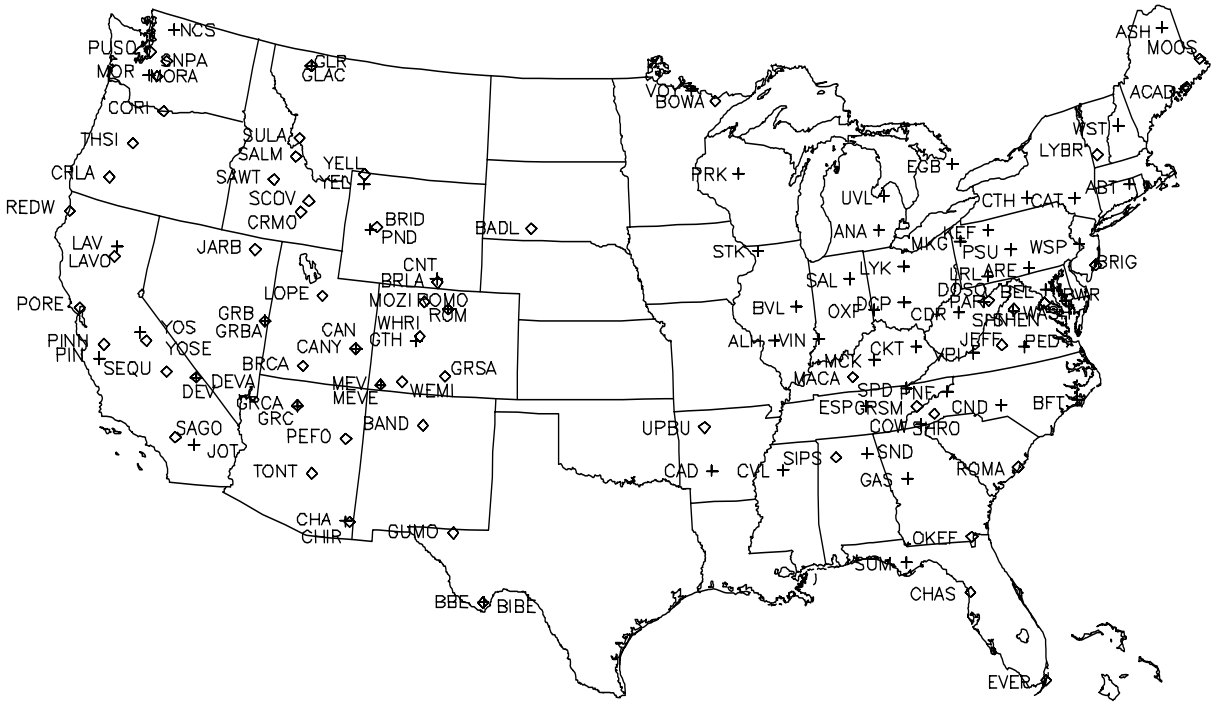

Figure A.1 *Map of monitoring sites, showing site abbreviations, from the IMPROVE network (diamonds) and the CDN (plusses) used in this analysis.*

IMPROVE organic carbon (OC), elemental carbon (EC), fine soil, and coarse mass (CM) are interpolated using a minimum curvature spline surface, which is appropriate for interpolation of the relatively low spatial density data set. (Isopleths of IMPROVE data interpolated using the spline method are shown in Chapter 2.5, and are similar to the interpolated fields used for this

analysis, although they correspond to a three-year period advanced one season from maps shown in this section). Concentrations for combined IMPROVE and CDN fields are interpolated using a nearest neighbor triangulation interpolation. The triangulation method provides more accurate interpolations than the spline method, in our opinion, for high density data sets. Maps shown in this section show contours of the triangulated fields. All interpolated fields, particularly at locations where estimates were made using interpolated data, were checked for reasonable behavior. For example, the IMPROVE site BRIG on the New Jersey coast, has high CM concentrations relative to other IMPROVE sites in the northeastern United States, likely due to sea salt. It is unlikely that this maritime CM extends inland any great distance, therefore BRIG was removed from the CM interpolation so as not to overestimate CM concentrations at neighboring, although more inland, CDN sites.

Mean CDN particle mass concentrations are converted to ambient pressure based on site elevation, although are not converted ambient temperature. IMPROVE data represent ambient sampling conditions. Sulfate and nitrate mass concentrations from both networks are converted to mass concentrations of fully neutralized ammonium salts. Due to an anticipated bias of CDN measurements to coarse particle nitrate, the three-year mean particle nitrate mass concentrations at 11 western CDN sites (PND, YEL, ROM, GRC, MEV, CAN, GRB, CHA, BBE, CNT, GTH) are adjusted to fine particle nitrate using a temperature and fine soil correlation model (Appendix G). Similar adjustments are not made to CDN nitrate data in other regions of the country, or for winter or summer data, because appropriate algorithms have not yet been developed.

Table A.1 *IMPROVE and CDN monitoring sites used in this analysis.*

IMPROVE			CDN		
Abbreviation	**State**	**Name**	**Abbreviation**	**State**	**Name**
ACAD	ME	Acadia NP	ABT	CT	Abington
BADL	SD	Badlands NP	ALH	IL	Alhambra
BAND	NM	Bandelier NM	ANA	MI	Ann Arbor
BIBE	TX	Big Bend NP	ARE	PA	Arendtsville
BOWA	MN	Boundary Waters CA	ASH	ME	Ashland
BRCA	UT	Bryce Canyon NP	BBE	TX	Big Bend NP
BRID	WY	Bridger WA	BEL	MD	Beltsville
BRIG	NJ	Brigantine NWR	BFT	NC	Beaufort
BRLA	WY	Brooklyn Lake	BVL	IL	Bondville
CANY	UT	Canyonlands NP	BWR	MD	Blackwater NWR
CHAS	FL	Chassahowitza NWR	CAD	AR	Caddo Valley
CHIR	AZ	Chiricahua NM	CAN	UT	Canyonlands NP
CORI	OR	Columbia River NSA	CAT	NY	Claryville
CRLA	OR	Crater Lake NP	CDR	WV	Cedar Creek
CRMO	ID	Craters of Moon NM	CHA	AZ	Chiricahua NM
DEVA	CA	Death Valley NP	CKT	KY	Crockett
DOSO	WV	Dolly Sods WA	CND	NC	Candor
EVER	FL	Everglades NP	CNT	WY	Centennial
GLAC	MT	Glacier NP	COW	NC	Coweeta
GRBA	NV	Great Basin NP	CTH	NY	Connecticut Hill
GRCA	AZ	Grand Canyon NP	CVL	MS	Coffeeville
GRSA	CO	Great Sand Dunes NM	DCP	OH	Deer Creek

Table A.1 *(Continued.)*

IMPROVE			CDN		
Abbreviation	**State**	**Name**	**Abbreviation**	**State**	**Name**
GRSM	TN	Great Smoky Mountains NP	DEV	CA	Death Valley NP
GUMO	TX	Guadalupe Mountains NP	EGB	ON	Egbert
JARB	NV	Jarbidge WA	ESP	TN	Edgar Evins
JEFF	VA	Jefferson NF	GAS	GA	Georgia Station
LAVO	CA	Lassen Volcanic NP	GLR	MT	Glacier NP
LOPE	UT	Lone Peak WA	GRB	NV	Great Basin NP
LYBR	VT	Lye Brook WA	GRC	AZ	Grand Canyon NP
MACA	KY	Mammoth Cave NP	GTH	CO	Gothic
MEVE	CO	Mesa Verde NP	JOT	CA	Joshua Tree NM
MOOS	ME	Moosehorn NWR	KEF	PA	Kane Exp. Forest
MORA	WA	Mount Rainier NP	LAV	CA	Lassen Volcanic NP
MOZI	CO	Mount Zirkel WA	LRL	PA	Laurel Hill
OKEF	GA	Okefenokee NWR	LYK	OH	Lykens
PEFO	AZ	Petrified Forest NP	MCK	KY	Mackville
PINN	CA	Pinnacles NM	MEV	CO	Mesa Verde NP
PORE	CA	Point Reyes NS	MKG	PA	M.K. Goddard
PUSO	WA	Puget Sound	MOR	WA	Mount Rainier NP
REDW	CA	Redwood NP	NCS	WA	North Cascades NP
ROMA	SC	Cape Romain NWR	OXF	OH	Oxford
ROMO	CO	Rocky Mountain NP	PAR	WV	Parsons
SAGO	CA	San Gorgonio WA	PED	VA	Prince Edward
SALM	ID	Salmon	PIN	CA	Pinnacles NM
SAWT	CO	Sawtooh NF	PND	WY	Pinedale
SCOV	ID	Scoville DOE Lab	PNF	NC	Cranberry
SEQU	CA	Sequoia NP	PRK	WI	Perkinstown
SHEN	VA	Shenandoah NP	PSU	PA	Penn State
SHRO	NC	Shining Rock WA	ROM	CO	Rocky Mountain NP
SIPS	AL	Sipsey WA	SAL	IN	Salamonie Reservoir
SNPA	WA	Snoqualmie Pass NF	SHN	VA	Shenandoah NP - Big Meadows
SULA	MT	Sula Peak	SND	AL	Sand Mountain
THSI	OR	Three Sisters WA	SPD	TN	Speedwell
TONT	AZ	Tonto NM	STK	IL	Stockton
UPBU	AR	Upper Buffalo WA	SUM	FL	Sumatra
WASH	DC	Washington, D.C.	UVL	MI	Unionville
WEMI	CO	Weminuche WA	VIN	IN	Vincennes
WHRI	CO	White River NF	VOY	MN	Voyageurs NP
YELL	WY	Yellowstone NP	VPI	VA	Horton Station
YOSE	CA	Yosemite NP	WSP	NJ	Washington Crossing
			WST	NH	Woodstock
			YEL	WY	Yellowstone NP
			YOS	CA	Yosemite NP - Turtleback Dome

NP = National Park
NM = National Monument
CA = Canoe Area
WA = Wilderness Area
NWR = National Wildlife Refuge
NSA = National Scenic Area
NS = National Seashore
NF = National Forest

A.2 RESULTS AND DISCUSSION

Combined IMPROVE and CDN nitrate, sulfate and b_{ext} maps for the three-year period, December 1995 through November 1998 are shown in Figures A.2 through A.4.

Figure A.2 is a map of mean particle nitrate mass concentrations, indicating maximum nitrate concentrations in excess of 3 $\mu g/m^3$ across the northern Midwest, with high particle nitrate concentrations also observed near some urban areas. Figure A.3 shows mean sulfate mass concentrations, indicating the highest mean sulfate mass concentrations, in excess of 7 $\mu g/m^3$ for the three-year period, occur at monitoring locations along the Ohio River and Tennessee Valleys. Note in Figure A.3 that the southeast boarder of the 7 $\mu g/m^3$ sulfate mass concentration contour reflects terrain features of the Appalachian Mountain chain.

Figure A.4 (also Figure 3.5 in Chapter 3.2.2) is a map of the reconstructed b_{ext} based on combined IMPROVE and CDN data. Mean reconstructed aerosol b_{ext} exceeds 120/Mm in a region of the eastern United States roughly corresponding to the region of maximum sulfate mass concentration shown in Figure A.2. Note that the region encompassed by the 120/Mm contour in the combined map is larger and has more spatial resolution than the same 120/Mm region based on IMPROVE data alone. Differences between some IMPROVE b_{ext} point values in Figure 3.4 compared to those in Figure 3.5 can be attributed to the different time periods for the respective maps, and the fact that F_T(RH) is calculated using Equation 3.17 at all sites in Figure 3.5, while in Figure 3.4 site specific values are used at some IMPROVE sites.

Comparison of mean IMPROVE and the CDN particle mass concentrations and b_{ext} values was performed at nearby monitoring sites. Table A.2 shows the root mean square (RMS) relative difference (expressed as a percent of the CDN mean) in means of sulfate and nitrate particle mass concentration, RH, and reconstructed b_{ext} for sites from the two networks within 50 km. These are a subset of the comparison sites in Appendix G, where sites separated by more than 50 km have been excluded, and the LYBR-LYE pair is excluded because data from LYE did not meet the minimum requirement for this analysis. The RMS difference for nitrate is higher than for sulfate, reflecting bias in the respective particle nitrate measurement from the two networks at the primarily western United States comparison sites. It is not surprising that the RMS difference for reconstructed b_{ext} is less than that of other quantities shown in Table A.2. Due to the proximity of comparison sites incorporated in RMS difference example, the same IMPROVE data are used in the reconstructed b_{ext} algorithm for quantities other than sulfate, nitrate, and RH.

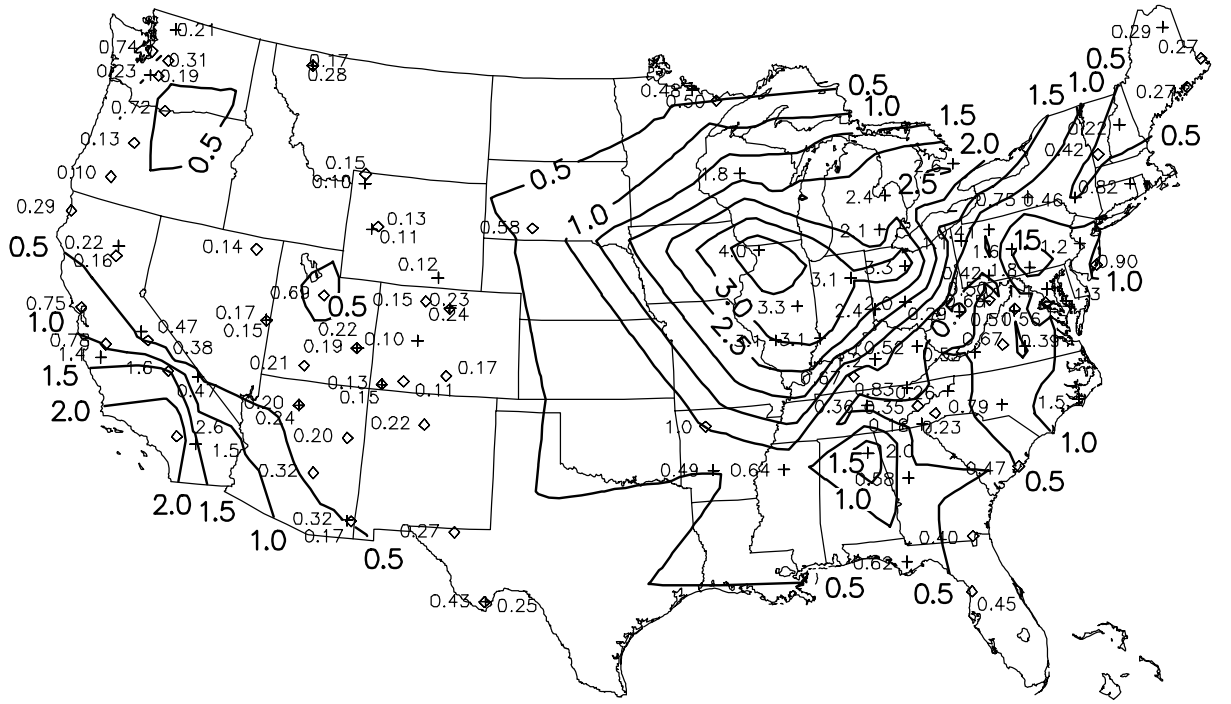

Figure A.2 *December 1995 through November 1998 mean particle nitrate (as ammonium nitrate) mass concentrations.*

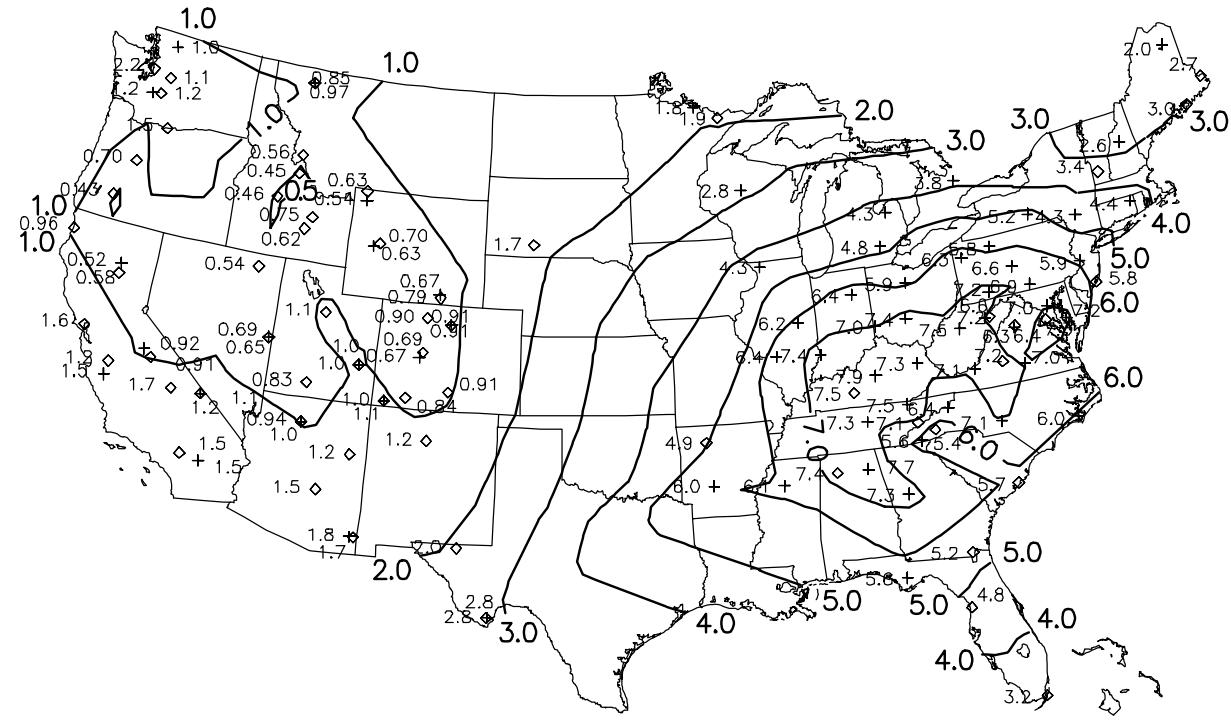

Figure A.3 *December 1995 through November 1998 mean particle sulfate (as ammonium sulfate) mass concentrations.*

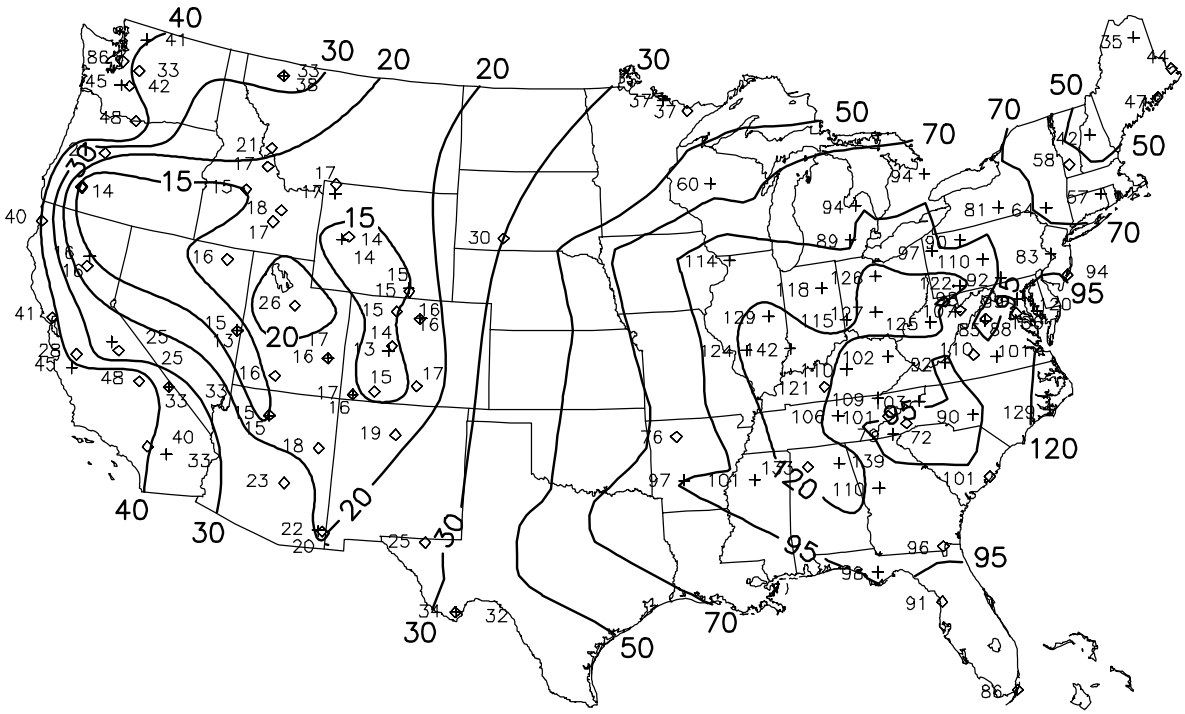

Figure A.4 *December 1995 through November 1998 mean reconstructed aerosol b_{ext}.*

Table A.2 *RMS percent difference for annual mean sulfate, nitrate, RH and reconstructed b_{ext} at nearby IMPROVE and CDN sites.*

Quantity	N	RMS Difference (%)
Sulfate	18	9
Nitrate	15	30
RH	15	9
Reconstructed b_{ext}	18	6

Seasonal maps of particle sulfate and nitrate mass concentration are shown in Figures A.5 through A.8. Figure A.5 indicates high wintertime particle nitrate concentrations throughout a large region of the northern Midwest, with maximum wintertime nitrate mass concentrations in excess of 4 $\mu g/m^3$ at CDN sites in Illinois, Indiana, and Ohio. This broad region of high particle nitrate mass concentrations is not captured by the IMPROVE Network. It is interesting to note the CDN site in Stockton, Illinois, which is not shown in Figure A.5 because the available data represent approximately 50% of the possible samples for the three-year winter period, has a wintertime mean particle nitrate mass concentration of 8 $\mu g/m^3$. Furthermore, Stockton, Illinois, nitrate data are shown in the map for three-year period (Figure A.2) because the data requirement specified for the entire three-year period are met at this site. Figure A.6 is a map of the wintertime mean sulfate mass concentration showing maximum values in excess of 4 $\mu g/m^3$ throughout much of the eastern United States. Higher wintertime sulfate concentrations are

confined generally east of the Appalachian mountains with a local minimum in the southeast United States at high elevation sites situated above the mixed layer for much of the winter.

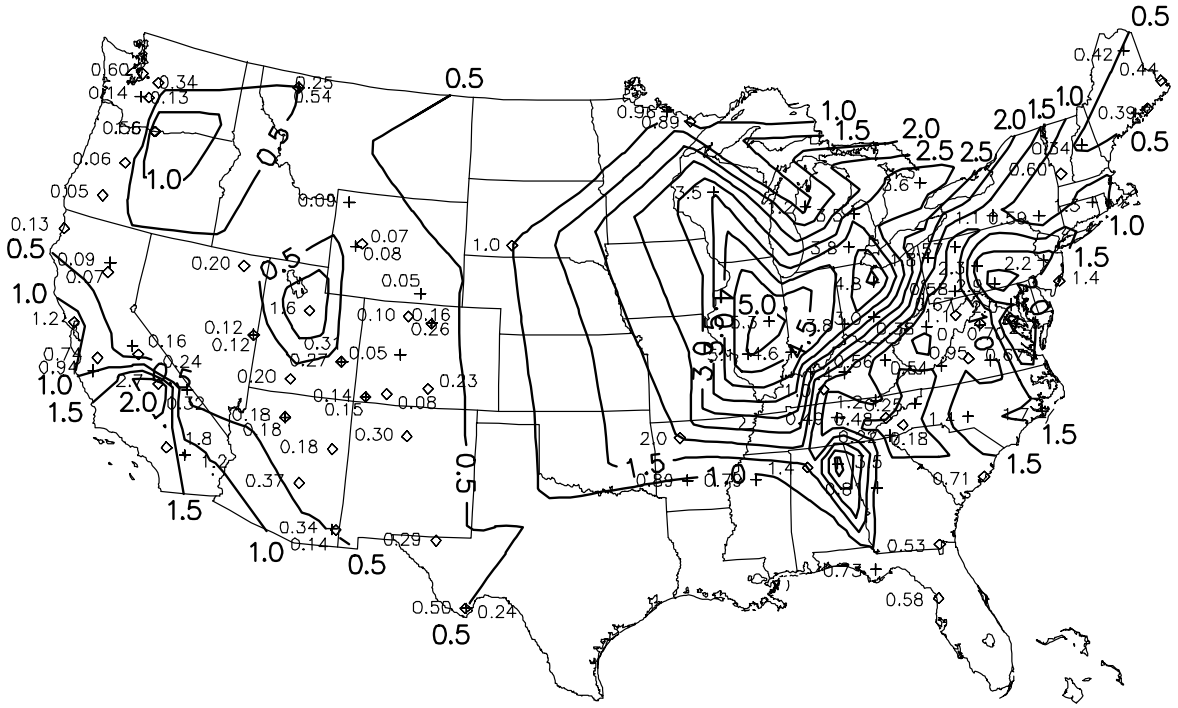

Figure A.5 *December 1995 through November 1998 mean winter particle nitrate mass concentrations.*

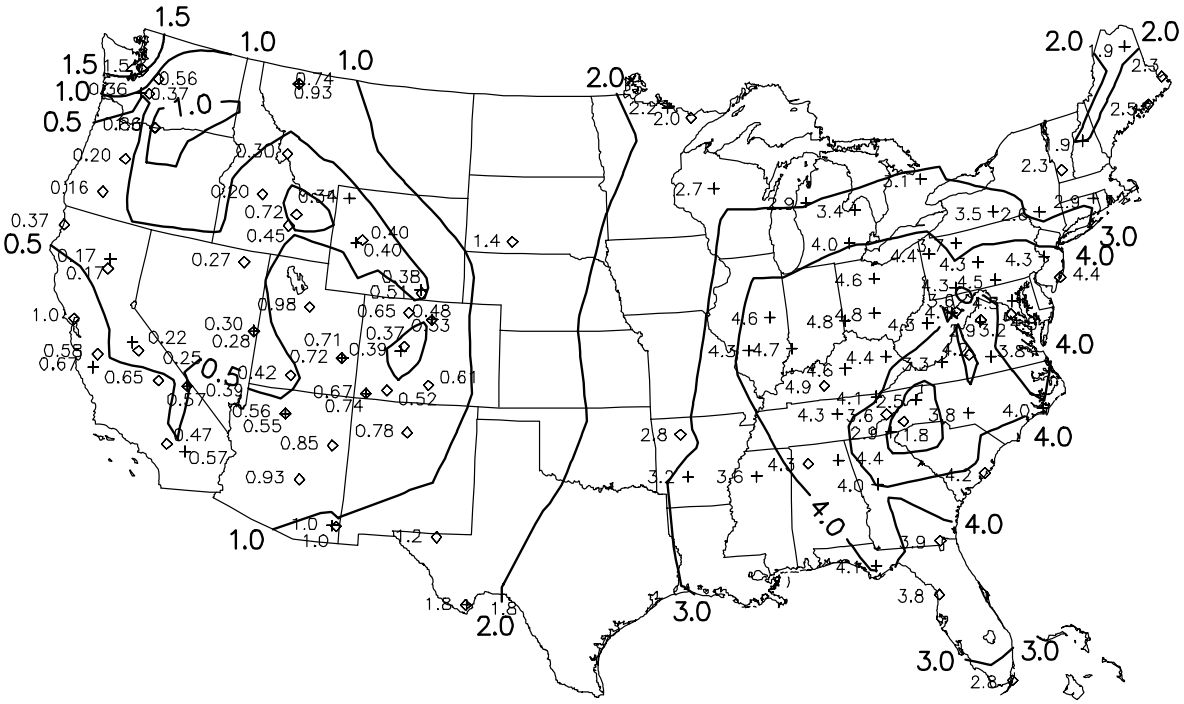

Figure A.6 *December 1995 through November 1998 mean winter sulfate mass concentrations.*

Figure A.7 is a map of summertime particle nitrate mass concentrations for the three-year period, showing values in excess of 1 $\mu g/m^3$ at some Midwest and California monitoring locations. It is interesting to note that the spatial pattern of particle nitrate seen during the winter, when particle nitrate mass concentrations are generally at a maximum, is essentially preserved in the summer nitrate map, although with lower magnitude. Figure A.8 is a map of mean summertime sulfate mass concentrations, showing maximum values in excess of 12 $\mu g/m^3$ centered over Kentucky and West Virginia, with steep decreasing concentration gradients in all directions away from the maximum. This contrasts with the winter sulfate map, where the region of maximum sulfate mass concentration in the eastern United States is comparatively broad, and mass concentration gradients exhibit a more gradual decline away from the highest wintertime values.

Figure A.9 is a map of reconstructed b_{ext} for the winter three-year period, showing many CDN sites in the northern Midwest with wintertime b_{ext} in excess of 100/Mm, generally corresponding to the region of high wintertime particle nitrate mass concentration. Wintertime b_{ext} is at a minimum (less than 10/Mm) in the western United States, Great Basin and Rocky Mountain regions, with local minimum b_{ext} in the eastern United States (less than 50/Mm) at a few high elevation sites along the Appalachian Mountain chain. Figure A.10 is a map of summertime b_{ext}, indicating a region of maximum b_{ext} (in excess of 170/Mm) along the Ohio River and Tennessee Valleys. The region of highest b_{ext} corresponds to monitoring sites where both sulfate and RH are high. For example, an increase in RH from 78% to 83% translates to a 31% increase in F_T(RH) as calculated by Equation 3.17. When the bulk of the light extinction budget is made up of hygroscopic chemical species, small changes in RH can have a strong influence on reconstructed b_{ext}, particularly at high RH values.

Table A.3 shows the RMS percent difference in winter sulfate, nitrate, and reconstructed b_{ext} and CDN and IMPROVE sites within approximately 50 km, while Table A.4 shows these values for the summertime comparison. Note that the sites used for the comparison are located primarily in the western United States and the large magnitude particle nitrate RMS difference likely reflects a sampling bias between IMPROVE and CDN specific to this region.

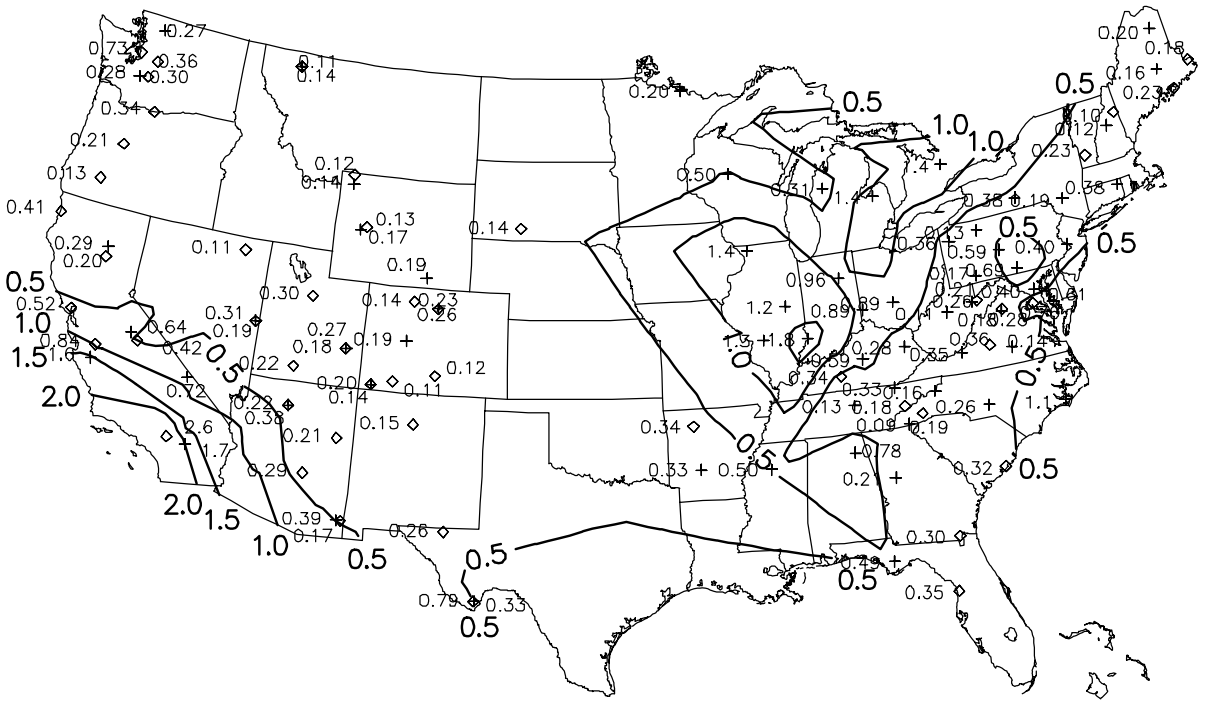

Figure A.7 *December 1995 through November 1998 mean summer particle nitrate mass concentrations.*

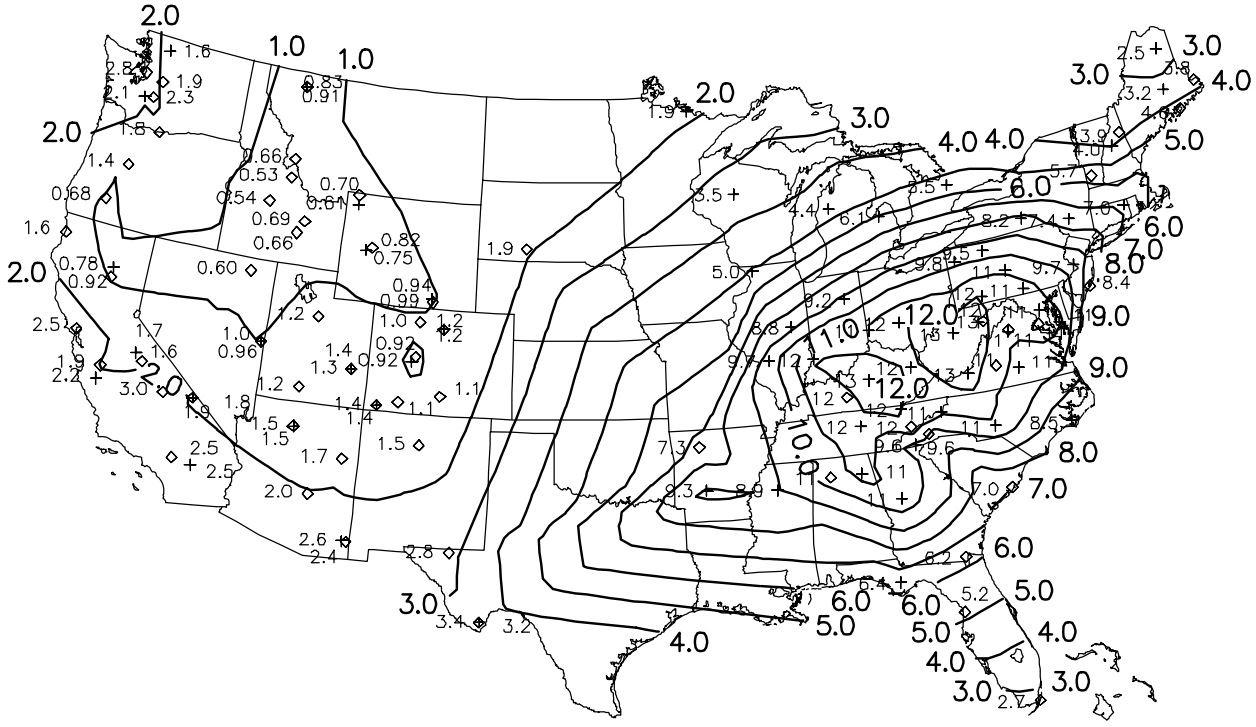

Figure A.8 *December 1995 through November 1998 mean summer sulfate mass concentrations.*

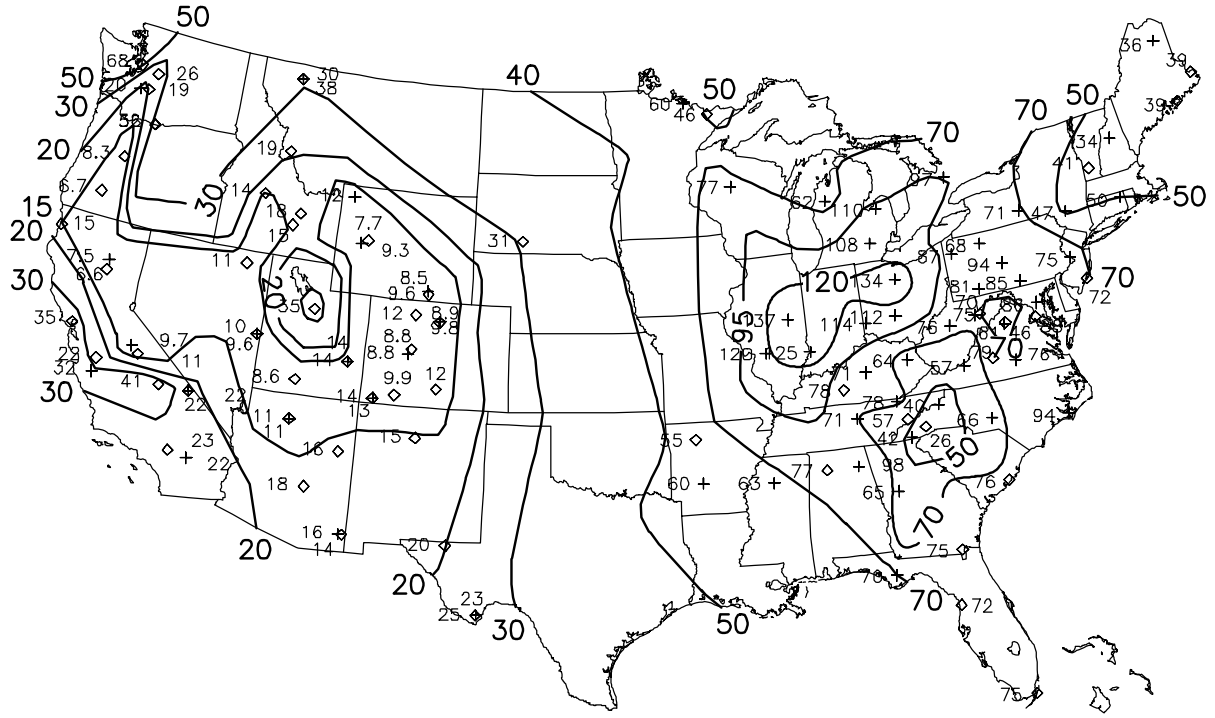

Figure A.9 *December 1995 through November 1998 mean winter reconstructed aerosol* b_{ext}.

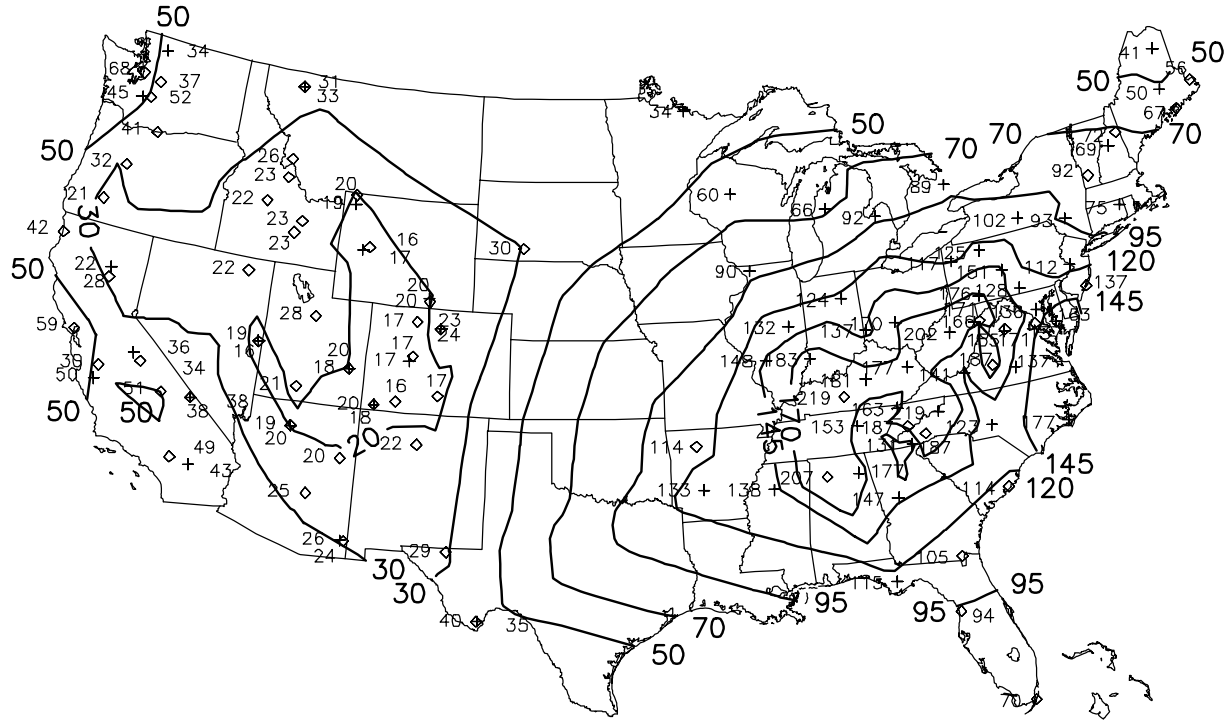

Figure A.10 *December 1995 through November 1998 mean summer reconstructed aerosol* b_{ext}.

Table A.3 *RMS difference for wintertime mean sulfate, nitrate, RH and reconstructed b_{ext} at nearby IMPROVE and CDN sites.*

Quantity	N	RMS difference (%)
Sulfate	17	14
Nitrate	14	43
RH	15	7
Reconstructed b_{ext}	17	12

Table A.4 *RMS difference for summertime mean sulfate, nitrate, RH and reconstructed b_{ext} at nearby IMPROVE and CDN sites.*

Quantity	N	RMS difference (%)
Sulfate	18	8
Nitrate	15	36
RH	18	10
Reconstructed b_{ext}	16	14

A.3 SUMMARY

Sulfate and nitrate particle mass concentrations from the CDN were combined with IMPROVE data to enhance spatial resolution of reconstructed aerosol b_{ext} maps. The spatial resolution of the combined b_{ext} maps in the eastern United States is greatly enhanced over maps based on IMPROVE data alone, particularly in the eastern United States where visibility conditions are traditionally the worst in the nation.

This analysis, which incorporates data from the three-year December 1995 through November 1998 period, illustrates that the haziest conditions in the United States occur in the Midwest and eastern United States, particularly along the Ohio River and Tennessee Valleys, in a region where mean b_{ext} exceeds 120/Mm. This region corresponds in general to the region of maximum sulfate mass concentration for the three-year period. Maximum summertime sulfate mass concentrations, in excess of 12 $\mu g/m^3$, center over Kentucky and West Virginia. These high summer sulfate mass concentrations, combined with mean RH values in excess of 80% at some sites, strongly influence spatial patterns of the summer b_{ext} maps, which exceeds 170/Mm across much of the eastern United States west of the Appalachian Mountains. Nitrates have a wintertime maximum particle mass concentration in excess of 4 $\mu g/m^3$ centered over Illinois, Indiana and Ohio, which corresponds to the regions of maximum wintertime b_{ext} in excess of 120/Mm.

In this analysis we assume sulfate and nitrate have the majority contribution to the particle light extinction budget at sites where b_{ext} is estimated using interpolated chemical mass concentration fields. This assumption likely holds at most eastern United States monitoring locations, where sulfates are major contributors to particle mass. The interpolations could be improved by incorporating factors such as terrain forcing, seasonal varying mixing heights, and measurements from sources other than IMPROVE to serve as basis for the interpolations, where

available. The disparity between IMPROVE and CDN particle nitrate mass concentration measurements remains troubling and should be further addressed, particularly in regions where particle nitrate mass concentrations are high and likely have a large contribution to b_{ext}. This type of analysis is also strongly influenced by RH, and could benefit from more refined and regionally specific estimates of the RH correction factor applied to hygroscopic aerosol species in the b_{ext} algorithm. Further applications of these combined b_{ext} data could be to refine regional chemical species b_{ext} budgets, or as a source of comparison data for b_{ext} maps estimated from human observations, or for comparison to remotely sensed estimates of aerosol optical depth in lower levels of the atmosphere.

A.4 REFERENCES

Ames R. B. and Malm W. C., Comparison of sulfate an nitrate particle mass concentrations from IMPROVE and CDN, submitted to *Atmospheric Environment*, 2000.

Chow, J. C.; Fujita, E. M.; Watson, J. G. ; Lu, Z., Lawson, D. R., Ashbaugh, L. L., Evaluation of filter-based aerosol measurements during the 1987 Southern California Air Quality Study, Environmental Monitoring and Assessment, *Environ. Monit. Assess.*, **30**(1):49-80, 1994.

Clean Air Status and Trends Network (CASTNet) Deposition Summary Report (1987-1995), EPA/600/R-98-207, July, 1998.

Falke S. F. and Husar R. B., Maps of $PM_{2.5}$ over the U.S. derived from regional $PM_{2.5}$ and surrogate visibility and PM_{10} monitoring data, Presented at the AWMA 90th annual meeting, 1998.

Hering S. and Cass G., The magnitude of bias in the measurement of $PM_{2.5}$ arising form volatilization of particulate nitrate from Teflon filters, *J. Air and Waste Management Association*, **49**(6):725-733, 1999.

Malm W. C., Sisler J. F., Huffman D., Eldred R. A., and Cahill T. C., Spatial and seasonal trends in particle concentration and optical extinction in the U.S. *J. Geophys. Res.* **99**(D1):1347-1370, 1994.

Sisler, J. F., *Spatial and Seasonal Patterns and Long Term Variability of the Composition of the Haze in the United States: An Analysis of Data from the IMPROVE Network,* Cooperative Institute for Research in the Atmosphere, Colorado State University, ISSN 0737-5352-32, 1996.

Sisler, J. F., Huffman, D., Latimer, D. A., Malm, W. C. and Pitchford, M. L., *Spatial and Temporal Patterns and the Chemical Composition of the Haze in the United States: An Analysis of Data from the IMPROVE Network 1988-1991*, Cooperative Institute for Research in the Atmosphere, Colorado State University, ISSN 0737-5352-26, 1993.